

# Multi-Level ML Based Burst-Aware Autoscaling for SLO Assurance and Cost Efficiency

Chunyang Meng, Haogang Tong, Tianyang Wu, Maolin Pan, and Yang Yu\*

**Abstract**—Autoscaling is a technology to automatically scale the resources provided to their applications without human intervention to guarantee runtime Quality of Service (QoS) while saving costs. However, user-facing cloud applications serve dynamic workloads that often exhibit variable and contain bursts, posing challenges to autoscaling for maintaining QoS within Service-Level Objectives (SLOs). Conservative strategies risk over-provisioning, while aggressive ones may cause SLO violations, making it more challenging to design effective autoscaling. This paper introduces BAScaler, a Burst-Aware Autoscaling framework for containerized cloud services or applications under complex workloads, combining multi-level machine learning (ML) techniques to mitigate SLO violations while saving costs. BAScaler incorporates a novel prediction-based burst detection mechanism that distinguishes between predictable periodic workload spikes and actual bursts. When bursts are detected, BAScaler appropriately overestimates them and allocates resources accordingly to address the rapid growth in resource demand. On the other hand, BAScaler employs reinforcement learning to rectify potential inaccuracies in resource estimation, enabling more precise resource allocation during non-bursts. Experiments across ten real-world workloads demonstrate BAScaler's effectiveness, achieving a 57% average reduction in SLO violations and cutting resource costs by 10% compared to other prominent methods.

**Index Terms**—Autoscaling, QoS, Burst, Resource Allocation, Services Computing.

## 1 INTRODUCTION

CLOUD computing is gaining traction, as evidenced by the widespread use of cloud-based software services or applications [1]. Until now, three main service models have fostered cloud adoption, namely Software, Platform, and Infrastructure as a Service (SaaS, PaaS, and IaaS) [2]. Among all these models, one of the pronounced benefits of the cloud is elasticity, which allows users to provision or de-provision resources provided by their applications on demand as workloads change [3]. It enables cloud subscribers to have a high degree of control over the virtualized resources, e.g., virtual machines (VMs) and containers, to adjust the amount of resources used flexibly, and to pay only for what has been used. Therefore, cloud computing reduces the cost to most cloud subscribers, from small businesses to large enterprises, and improves the resource utilization that is often low in the past [4].

However, enterprises experience fluctuations in business loads due to rapid changes and fierce competition in the market environment. When the business load fluctuates, manually adjusting the number of resources at the earliest opportunity is necessary [6]. Otherwise, the service performance may be compromised when the business load increases, or resources may be wasted when the business load decreases. Manual adjustments to resource provisioning are complex and need more real-time assurance [4]. The desire to overcome this issue motivates the appearance of

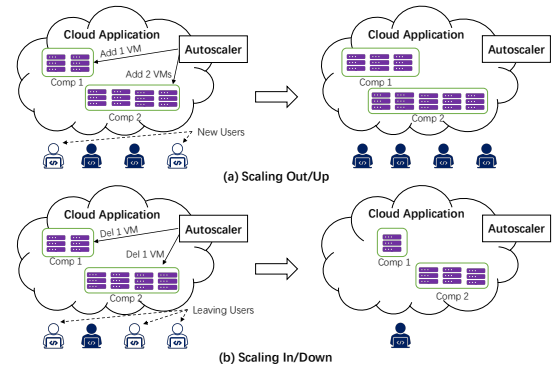


Fig. 1. Typical autoscaling scenarios—right sizing of resources. (a) Increased requests lead to congestion, prompting the autoscaler to either scale out (adding VMs) or scale up (boosting resources in existing VMs). (b) Decreased requests trigger deprovisioning actions, such as scaling in (removing VMs) or scaling down (reducing resources in existing VMs). Source: This figure adapted from Chenhao Qu (2018) [5].

the autoscaling technique, as shown in Fig. 1, which can autonomously and dynamically provision and de-provision a set of resources to cater to fluctuant application workloads without human intervention so that the resource consumed is minimized and QoS is maintained [5].

Given the dynamic and uncertain nature of the shared cloud infrastructure, the autoscaling system has been engineered as one of the most complex, sophisticated, and intelligent artifacts created by humans, aiming to achieve fine-grained, self-adaptive, and dependable runtime scaling [7]. Existing autoscaling methods (e.g., reactive [8]–[10], proactive [11]–[14], and hybrid methods [15]–[18]) guarantee QoS and/or reduce cost primarily by dynamically assigning the right amount of computational resources using handcrafted

- C. Meng, H. Tong, and T. Wu are with the School of Computer Science and Engineering, Sun Yat-sen University, Guangzhou, China.  
E-mail: {mengchy3, tonghg, wuty26}@mail2.sysu.edu.cn.
- M. Pan and Y. Yu are with the School of Software Engineering, Sun Yat-sen University, Zhuhai, China.  
E-mail: {panml, yuy}@mail.sysu.edu.cn.

Manuscript received February 20, 2024.  
(Corresponding author: Yang Yu.)

heuristics, queueing theory, control theory, and machine learning algorithms. Unfortunately, as described in §2.2, these works generally lack in-depth consideration of the complex scenarios. For example, most of them are oblivious to workload bursts and lack targeted solutions, making them vulnerable to bursts [19]. Moreover, estimating resources with only a single model (e.g., performance model) or a static policy (e.g., rule-based or heuristic) lacks robustness since these methods may be inaccurate, especially in uncertain cloud environments, leading to incorrect scaling decisions [20].

**The BAScaler.** To this end, we present BAScaler, a Robust Burst-aware Autoscaling framework for fine-grained containerized cloud services or applications. It seeks to automatically re-provision resources by considering workload bursts and estimating resources using combinatorial multi-level ML models, thus optimizing QoS assurance and cost efficiency in time-varying workloads. BAScaler achieves its goal primarily through four components: *Workload Prediction*, *Burst Detection & Handling*, *Resource Estimation*, and *Estimation Enhancement*.

Firstly, the *Workload Prediction* module forecasts the range of future workload based on historical data. Then, the *Burst Detector & Handler* module identifies bursts by comparing the forecasted range with the ground truth and provides an appropriate estimation of burst intensity. Based on whether a burst occurs or not, BAScaler adopts different resource allocation strategies. For burst scenarios, BAScaler utilizes an Autoregressive (AR) model with short-term trend capture capabilities to generate an appropriate overestimation through the Bootstrapping method and then combines the Support Vector Regression (SVR) driven performance models for resource estimation. For non-burst scenarios, BAScaler employs the performance models for initial resource estimation and then jointly uses deep reinforcement learning (DRL) to correct possible inaccuracy estimation dynamically. Finally, based on the estimated resources, BAScaler proactively allocates resources before workload changes to guarantee SLAs and reduce costs. If the prediction results are unsatisfactory, the DRL can also autonomously perform reactive autoscaling based on the current state.

**Contributions.** To the best of our knowledge, this is the first work to provide hybrid autoscaling for fine-grained containerized cloud software services or applications to optimize QoS assurance and cost efficiency by considering bursts and using robust resource estimation in a workload-pattern-agnostic way with multi-level ML models. Generally, our main contributions are:

- 1) **Burst Detection & Handling:** We propose a new mechanism for burst detection and handling, which treats workloads that do not conform to predictions as bursts. Moreover, we utilize the AR model and *Bootstrapping* to obtain an appropriate overestimation of burst intensity, providing valuable references for resource planning.
- 2) **Estimation Enhancement:** We propose a novel method for enhancing resource estimation. It improves the accuracy and robustness of resource allocation by dynamically correcting potentially inac-

curate estimation results using DRL agent and real-time telemetry data.

- 3) **Burst-Aware Autoscaling:** On this basis, we propose a robust burst-aware autoscaling framework, named BAScaler, which takes targeted resource planning based on whether the workload is bursty and allocates resources accordingly, optimizing SLO assurance and cost efficiency on fluctuating workloads.
- 4) **Implementation & Evaluation:** We design and implement the BAScaler prototype and validate BAScaler in both simulation and real-world environments using realistic workloads with different characteristics. The experimental result demonstrates that BAScaler is a promising approach.

The rest of this paper is organized as follows. Section 2 introduces the background and motivation. Section 3 describes the problem formulation of BAScaler, followed by the system design. The basic idea and detailed design are presented in Section 4. Section 5 delineates the experimental setup and presents the results obtained. Some discussions on the generality and limitations of BAScaler is conducted in Section 6. The related work is examined in Section 7, followed by the conclusion of this study in Section 8.

## 2 BACKGROUND AND MOTIVATION

### 2.1 Background

**ML Technology.** Machine learning (ML) is the key technology for implementing artificial intelligence [21]. From data analysis to automated processes, ML is reshaping the way we leverage information in the digital age. ML-powered systems have the potential to streamline operations, enhance decision-making processes, and drive innovation across organizations. ML-powered predictive analytics enables organizations to forecast trends, anticipate customer needs, and optimize resource allocation.

Common ML techniques include traditional statistical ML, deep learning (DL), and reinforcement learning (RL). Traditional statistical ML models [22], such as SVM and K-Means, typically rely on specific statistical principles and mathematical models. Through supervised or unsupervised learning, these models can extract patterns and regularities from relatively small historical data. DL [23], exemplified by models like Transformer, represents a ML approach based on neural network structures. By performing multilayered nonlinear transformations, it acquires a robust capacity for nonlinear modeling. RL [24], with corresponding models like PPO, is a method for teaching agents how to make decisions through interactions with the environment. Suited for dealing with uncertain environments and scenarios requiring long-term decision-making, reinforcement learning emphasizes reward signals and sequential decision-making.

**Workload Characteristics.** The large-scale social behaviour inherent in software applications or services leads to variations and diversity in workload intensity and characteristics [25]. Some workloads exhibit repetitive patterns, exemplified by Google Search workload [26], which displays a daily cycle with higher request arrival rates during the day compared to nighttime. Alternatively, some workloads showcase seasonal variations; for instance, the workload

of an online store may experience a substantial surge preceding Christmas. Moreover, sporadic spikes and bursts may occur due to isolated events, such as when Michael Jackson passed away, resulting in a notable spike directed to Wikipedia for articles related to him. On the other hand, some workloads exhibit weak or no patterns, such as the FIFA World Cup workload [27], primarily associated with unpredictable World Cup-related activity and user behavior.

The characterization of workloads presents a challenging endeavor due to the multitude of parameters available for such characterization. Regarding prediction and elasticity, two primary characteristics significantly impacting workload performance are periodicity and burstiness [28]. Periodicity, often assessed using autocorrelation, entails the examination of a signal's cross-correlation with a time-shifted iteration of itself [29]. Burstiness, while lacking a prevailing method for measurement, has been approached through various techniques [30]. Gusella [31] suggested the use of the index of dispersion, while Minh et al. [32] advocated for the application of normalized entropy.

## 2.2 Motivation

As mentioned earlier in the section of introduction, although there have been some studies on autoscaling, they lack more careful considerations on different workload characteristics, limiting the performance of their algorithms. To better understand the impact of dynamic workloads on auto-scaling, we have conducted extensive auto-scaling experiments in a public cloud environment using 10 real workloads with different characteristics. Our key insights are as follows.

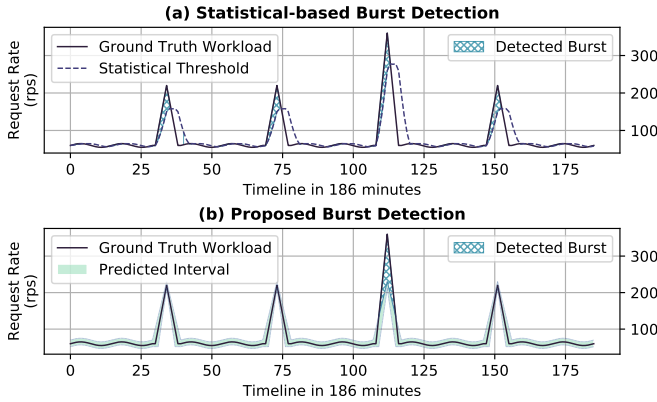


Fig. 2. An example illustrates the comparison. The proposal will not identify periodic workload spikes as bursts. Other statistical methods primarily differ in statistical threshold  $ST_w$ . Here, the  $ST_w = MA_w + 0.6 \times std_w$  presented in [33], where  $MA_w$  and  $std_w$  represent the moving average and the standard deviation of the workload over the last  $w$  time steps, respectively.

**Motivation ①: Diverse workload characteristics need to be considered.** Several prior works always make the assumption that the workload of cloud applications follows a fixed pattern, forming the basis for automated scaling decisions. For instance, reactive scaling methods assume infrequent workload fluctuations, while proactive scaling methods based on predictions assume workload adherence to predictable cyclic patterns. However, through automated scaling based on ten real workloads, we discovered that

these assumptions do not hold in practice. Characteristics of real cloud workloads are often time-varying, accompanied by multiple features, and different workload types exhibit distinct characteristic patterns. Incorrect assumptions can render resource allocation ineffective in unexpected workloads, impairing the performance of automated scaling and impacting request response times. Therefore, it is imperative for automated scaling methods to account for the various characteristics of workloads. Furthermore, we observed that most workloads are predictable, while accurately predicting sudden requests through analysis proves challenging.

**Motivation ②: bursty workloads damage the QoS severely.** As a salient workload characteristic, the burstiness critically impacts resource provisioning and the performance of cloud-based applications [25]. They can quickly exceed the available resources and cause performance issues or downtime. For example, suppose a web application experiences a sudden surge in user traffic due to a viral social media post. In that case, it may overwhelm the cloud infrastructure resources, leading to slow response times or website crashes. Therefore, it is necessary to cope with workload bursts properly to avoid damage to the QoS. However, the bursts are caused by flash events or crowds, meaning that the timing and amount of bursts can be stochastic. Currently, there is yet to be a practical solution to predict bursts before they happen, and we can only detect and handle them reactively to the best of our abilities. A few works focus on bursts [19], [34], but the burst detection algorithms in these works use statistical (e.g., moving average [33], [35], [36], entropy [30]) based approaches, which detect bursts by quantifying how much the workload fluctuates. They will mislabel predictable workload spikes as bursts, thus affecting overall performance. Fig. 2 depicts an example of a comparison between the proposed prediction-based burst detection algorithm and a statistics-based burst detection algorithm. The statistics-based approach detects bursts by quantifying the degree of workload fluctuation and will identify periodic workload spikes as bursts. While the proposal identifies workload spikes that do not match the prediction intervals as bursts, it effectively distinguishes between actual bursts and periodic workload spikes.

**Motivation ③: Trend towards fine-grained resource allocation.** Nowadays, cloud computing continues to evolve along with its increasing adoption. Throughout the evolution, not only have the aforementioned models advanced and new ones emerged, but also the technologies in which this paradigm is based (e.g., virtualization) have continued to progress. For instance, the use of novel virtualization techniques such as containers that enable improved utilisation of the physical resources and further hide the complexities of hardware is becoming increasingly widespread, even leading to a new service model being offered by providers known as container as a service (CaaS). There has also been a rise of function as a service (FaaS) that aid industries in creating value by being easily configured to meet specific business requirements. As an example, AWS Lambda employs lightweight containers to execute functions and dynamically creates and destroys container instances upon function triggers, which frees developers from the burden of resource management and complex configurations. As we can see through the history, the granularity of vir-

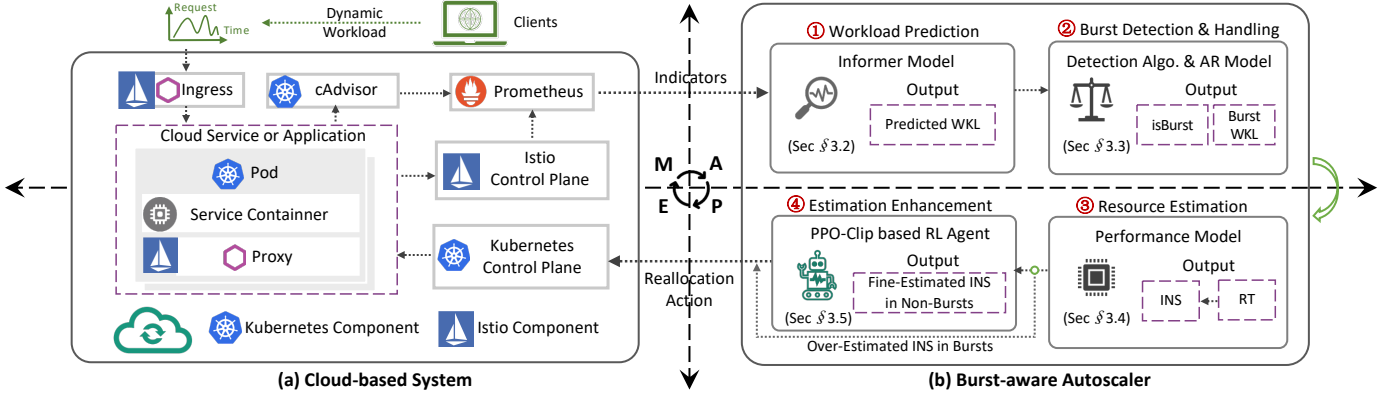


Fig. 3. Overview of the BAScaler shown as a MAPE loop: (a) Cloud-based system that provides Monitoring and Execution; (b) Burst-aware autoscaler for Analysis and Planning includes *Workloads Prediction*, *Burst Detection & Handling*, *Resource Estimation*, and *Estimation Enhancement*.

tualization has been reduced gradually from machine to function with the evolution from VM-based platforms to the serverless platform. Compared with traditional VM-based auto-scaling, container-based autoscaling is inherently more granular and lightweight, and containerised workloads may come with more stringent time constraints such as task deployment latency, task completion time, and communication latency.

### 3 THE BASCALER

#### 3.1 System Overview

The overview of the BAScaler framework is presented in Fig. 3, following a typical MAPE loop: Monitoring (M), Analysis (A), Planning (P), and Execution (E). We delegate monitoring and execution to cloud-hosted third-party software or call the cloud provider's API. This paper focuses on the analysis and planning phases, with Algorithm 1 describing the workflow of the Burst-aware Autoscaler.

- **Monitoring.** In monitoring phase, BAScaler needs to systematically monitor certain performance metrics to determine the necessity and methodology for scaling operations (shown at the top of Fig. 3(a) and described in Line 5 of Algorithm 1). Specifically, BAScaler uses the cAdvisor, integrated into the Kubernetes, to monitor the applications and collect metrics at the container layer, including CPU utilization, memory usage, etc. In addition, it uses Istio to generate detailed telemetry for all service communications and collect metrics at the application layer (e.g., request rate and average response time). The collected metrics are stored in Prometheus, a time series database, for querying.
- **Analysis.** In analysis phase, the collected performance metrics undergo further processing to unveil latent information crucial for determining scaling operations. BAScaler first uses the monitored workloads and the Informer model with long-term patterns capture capabilities to predict the range of future workloads (marked as ①, described in Line 6, and details in §3.2). Based on the prediction results, real-time comparison between the predicted and actual workloads is then conducted to detect bursts

(marked as ②, described in Line 7, and details in §3.3). Once the burst is detected, BAScaler utilizes an AR model with short-term trend capture capabilities to generate an appropriate overestimation via Bootstrapping method (marked as ②, described in Lines 8-10, and details in §3.3).

- **Planning.** The planning phase estimates the total amount of resources that should be allocated in the next scaling action. Based on whether a burst occurs or not, BAScaler adopts different resource estimation methods. For bursts, BAScaler utilizes performance models, the overestimated burst workloads, and performance constraints (i.e., SLO) to generate a relatively generous amount of resources (marked as ③, described in Line 11, and details in §3.4). For non-bursts, BAScaler employs the performance model for initial resource estimation and then jointly deep reinforcement learning to correct possible inaccuracy estimation dynamically (marked as ④, described in Lines 12-14, and details in §3.5).
- **Execution.** The execution phase provision or deprovision the resources based on the scaling plan (shown at the bottom of Fig. 3(a) and described in Line 15). It is straightforward, and we implemented it by calling the Kubernetes API [37].

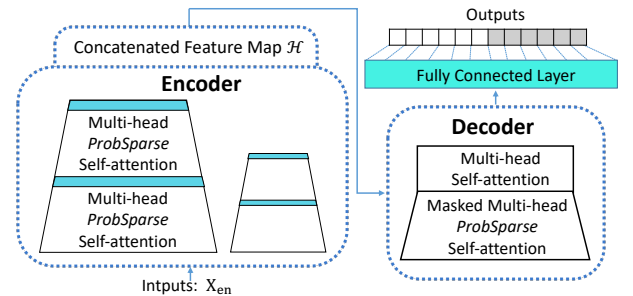


Fig. 4. Structure of *Informer*

#### 3.2 Workload Predictor

As one of the core components, the workload predictor aims to accurately predict all non-bursty or predictable

**Algorithm 1** BAScaler's Autoscaling

---

```

1: Initialize workload predictor  $Q$  with trained weights  $\sigma$ 
2: Initialize performance model  $P$  with trained weights  $\omega$ 
3: Initialize DRL policy  $\pi_\theta$  with trained parameters  $\theta$ 
4: while not done do
5:   Observe  $S_t = \{ins_t, cpu_t, mem_t, wkl_t\}$  and time-series workload  $X_t = \{wkl_{t-M}, \dots, wkl_{t-1}, wkl_t\}$ 
6:   Predict workload  $\hat{Y}_t = Q_\sigma(X_t)$  and set  $wkl_t = \hat{Y}_t[1][0]$ 
7:   Detect burst isBurst by Algo. 2 using  $\hat{Y}_t$ 
8:   if isBurst then
9:     Overestimate bursty workload by AR model, and set to  $wkl_t$ 
10:  end if
11:  Estimate resource  $ins_t$  by:
     $\arg \max_{INS} P_\omega(RT|INS, WKL = wkl_t), s.t. RT < SLO_{rt}$ 
12:  if not isBurst then
13:    Enhance resource estimation by PPO policy:
       $ins_t = A_t = \pi_\theta(a|s = S_t)$ 
14:  end if
15:  Allocate resource by  $ins_t$ 
16:  Wait until next time step, and set  $t = t + 1$ 
17: end while

```

---

workloads. The prediction result will serve as an essential basis for burst detection and resource planning. At each discrete time step  $t = 1, 2, \dots$ , the input,  $\mathcal{X}^t = \{X_1^t, \dots, X_{L_x}^t\} \in \mathbb{R}^{L_x \times 2}$ , to the predictor is the time-series workloads observed in the past  $L_x$  time slices at time  $t$ , where  $X_i^t = \{WL^{t-L_x+i}, TS^{t-L_x+i}\}$  contains the observed workload sequence and its corresponding timestamp at time step  $t - L_x + i$ . The basic problem here is forecasting the workload at time step  $t + 1$ . Considering the poor fault tolerance of a single predicted value as the basis for subsequent burst detection module decisions. It is better to predict the workload interval,  $\hat{\mathcal{Y}}_t = \{\hat{Y}_1^t, \dots, \hat{Y}_{L_y}^t\} \in \mathbb{R}^{L_y \times 3}$ , for the next  $L_y$  time steps:

$$\{\hat{Y}_1^t, \dots, \hat{Y}_{L_y}^t\} = F(\{X_1^t, \dots, X_{L_x}^t\}; \omega) \quad (1)$$

where  $\hat{Y}_i^t = \{\hat{y}_{low}^{t,i}, \hat{y}_{median}^{t,i}, \hat{y}_{up}^{t,i}\}$  contains the predicted minimum, median and maximum of workloads.  $F(\cdot; \omega)$  denotes the forecast function with parameter  $\omega$ .

Since cloud workloads are associated with specific business or user-related activities, there may be daily, weekly, or monthly fluctuations in workload. These cyclic patterns create long-range dependencies in the workloads. To capture long-range dependencies, we build such a workload predictor through Informer [38], a deep learning model specifically designed for time series forecasting, with the following modules.

**Workload Representation.** Before the original workload can be fed into the *Informer* model for forward inference, the original workload must first be embedded with global position information and temporal information so that the workload's sequential features and time-related features can be characterized. Assume the timestamp context (i.e.,  $TS$ ) have  $P$  types of global timestamps (e.g., hour, day, week, and month), and the feature dimension after all embedding operations is  $d_{model}$ . The position embedding and stamp

embedding methods are shown as Eqs. (2) and (3), respectively:

$$\begin{aligned} PE_{(pos, 2j)} &= \sin(pos / (2L_x)^{2j/d_{model}}), \\ PE_{(pos, 2j+1)} &= \cos(pos / (2L_x)^{2j/d_{model}}), \quad j \in \{1, \dots, \lfloor d_{model}/2 \rfloor\} \end{aligned} \quad (2)$$

$$SE_{(pos, p)} = h_{(pos, p)} / (L_{(pos, p)} - 1) - 0.5 \quad (3)$$

where  $h_{(pos, p)}$  and  $L_{(pos, p)}$  denote the value of temporal type  $p$  and its period for the  $pos$ -th data of the input, respectively. Taking the hour-in-day as an example, suppose the corresponding hour information in the current timestamp to be processed is 5 am, then the corresponding  $h = 5$  and  $L = 24$ .

To align the dimension, the scalar contexts (i.e.,  $WL$ ) are mapped to  $d_{model}$ -dim vectors  $\mathbf{u}_i^t$  by passing them through 1-D convolutional filters with kernel width=3 and stride=1. Thus, we have the feeding vectors:

$$\mathcal{X}_{feed}^t[i] = \mathbf{u}_i^t + PE_{(t-L_x+i, \cdot)} + \sum_{p \in P} SE_{(t-L_x+i, p)}, \quad i \in \{1, \dots, L_x\} \quad (4)$$

These feeding vectors are then shaped into a matrix  $\mathbf{X}_{en}^t \in \mathbb{R}^{L_x \times d_{model}}$ .

**Encoder-Decoder.** As shown in Fig. 4, the feeding matrix  $\mathbf{X}_{en}^t$  is then passed through an encoder and decoder modules to generate the forecasted workload. The encoder's primary role is to analyze and extract relevant features from feeding matrix  $\mathbf{X}_{en}^t$  and encode it into a hidden state representation  $\mathcal{H}^t = \{\mathbf{h}_1^t, \dots, \mathbf{h}_{L_h}^t\}$ . The encoder contains a 3-layer stack and a 1-layer stack (1/4 input), and each stack forwards from  $j$ -th layer into  $(j+1)$ -th layer as:

$$\mathbf{X}_{j+1}^t = \text{MaxPool}(\text{ELU}(\text{Conv1d}([\mathbf{X}_j^t]_{AB}))) \quad (5)$$

where  $[\cdot]_{AB}$  represents the *Multi-head ProbSparse Self-attention* layer [38].  $\text{Conv1d}(\cdot)$  performs a 1-D convolutional filters (kernel width=3) on time dimension with the  $\text{ELU}(\cdot)$  activation function. Then a max-pooling layer  $\text{MaxPool}(\cdot)$  with stride=2 downsample  $\mathbf{X}^t$  into its half slice after stacking a layer. The final hidden representation of the encoder is the concatenation of all the stacks' outputs.

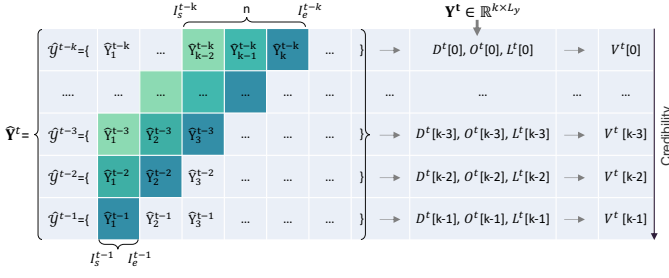
Then the decoder module decodes  $\mathcal{H}^t$  into an output representation  $\hat{\mathcal{Y}}^t$ . It is composed of a stack of two identical multi-head attention layers. Masked multi-head attention is applied in the *ProbSparse* self-attention computing by setting masked dot products to  $-\infty$ . Then a fully connected layer acquires the final output. We choose the quantile loss function on result w.r.t the workload prediction, as it can compute the loss between ground truth  $\mathcal{Y}^t = \{y^{t,1}, \dots, y^{t,L_y}\}$  and the prediction  $\hat{\mathcal{Y}}^t$  in given quantiles  $Q$ :

$$\mathcal{L}_q(y, \hat{y}) = q \times \max(y - \hat{y}, 0) + (1 - q) \times \max(\hat{y} - y, 0) \quad (6)$$

$$\mathcal{L}_Q(\mathcal{Y}^t, \hat{\mathcal{Y}}^t) = \frac{1}{|Q|} \sum_{i=1}^{L_y} \sum_{q \in Q} \mathcal{L}_q(y^{t,i}, \hat{y}_q^{t,i}) \quad (7)$$

In our experiments, the joint loss of the prediction interval's upper, median, and lower bounds can be calculated by setting  $Q = \{0.1, 0.5, 0.9\}$ . Moreover, the parameters are optimized by *Stochastic Gradient Descent* (via *Adam*) that propagated back the loss from the decoder's outputs across the entire model.



Fig. 5. Calculation process of  $V^t$ 

### 3.3 Burst Detector and Handler

The burst detector and handler component is designed to detect bursty workloads and provide an effective way to handle them accordingly.

**Burst Detection.** The burst detector receives the predictions for the past  $k$  time steps  $\hat{\mathbf{Y}}^t = \{\hat{\mathbf{Y}}^j = \{\hat{Y}_1^j, \dots, \hat{Y}_{L_y}^j\} | j \in [t-k, t-1]\} \in \mathbb{R}^{k \times L_y \times 3}$  and compares them with the ground truths  $\mathbf{Y}^t = \{\mathbf{Y}^i = \{y^{j,1}, \dots, y^{j,L_y}\} | j \in [t-k, t-1]\} \in \mathbb{R}^{k \times L_y}$  to determine whether the workload at time  $t$  is bursty. Its basic principle for determining the workload for the current time as the burst is that the degree of the ground truth deviates from the multi-step prediction interval is greater than the given thresholds. For this purpose, we designed  $D^t \in \mathbb{R}^k$  and  $O^t \in \mathbb{R}^k$  to quantify the deviation distances and the number of deviations for each  $y^j - \hat{y}^j$  pair in the last  $k$  time steps, respectively:

$$D^t = \left\{ \frac{1}{I_e - I_s + 1} \sum_{i=I_s}^{I_e} d(\hat{Y}_i^j, y^{j,i}) \mid j \in [t-k, t-1] \right\} \quad (8)$$

$$O^t = \left\{ \sum_{i=I_s}^{I_e} (d(\hat{Y}_i^j, y^{j,i}) > 0) \mid j \in [t-k, t-1] \right\} \quad (9)$$

where  $I_s^j$  and  $I_e^j$ , defined in Eq. (10), denote the starting and ending indexes of the  $y^{j,\cdot} - \hat{Y}^j$  pair that need to be calculated at time  $j$ , respectively.  $d(\cdot, \cdot) \geq 0$  is defined in Eq. (11). When the truth is within the prediction interval, then  $d(\cdot, \cdot) = 0$ . Conversely,  $d(\cdot, \cdot) > 0$  is called an outlier, and its value reflects the relative distance between the outlier and the prediction interval.

$$I_e^j = t - j; \quad I_s^j = \begin{cases} 1, & \text{if } I_e^j \leq n \\ I_e - n + 1, & \text{else} \end{cases}; \quad j \in [t-k, t-1] \quad (10)$$

$$d(\hat{Y}_i^j, y^{j,i}) = \text{ReLU}(y^{j,i} - \hat{y}_{up}^{j,i}) / \hat{y}_{up}^{j,i} + \text{ReLU}(\hat{y}_{low}^{j,i} - y^{j,i}) / \hat{y}_{low}^{j,i} \quad (11)$$

$$L^t = \left\{ \frac{1}{I_e - I_s + 1} \sum_{i=I_s}^{I_e} \mathcal{L}_q(y^{j,i}, \hat{y}_q^{j,i}) \mid q = 0.5, j \in [t-k, t-1] \right\} \quad (12)$$

Similarly, the prediction errors  $L^t \in \mathbb{R}^k$  (Eq. (12)) can also reflect the degree of difference between the prediction and truth. Thus, we have the proposals for whether the workload at time  $t$  is bursty:

$$V^t = \{(D^t[i] > \lambda_d \text{ and } O^t[i] \geq n/2) \text{ or } L^t[i] > \lambda_l \mid i \in [0, k]\} \quad (13)$$

where  $\lambda_l$  and  $\lambda_d$  are preset thresholds for controlling the sensitivity of burst detection.  $V^t[i] = 1/0$  indicates that the

prediction  $\hat{y}^{t-k+i}$  suggests that the current workload (i.e., time step  $t$ ) is/isn't bursty. For clarity, Fig. 5 presents the calculation of  $V^t$ .

As shown in Algorithm 2, our burst detection algorithm first initializes  $D^t, O^t, L^t$ , and  $V^t$  according to the above equations (Lines 1-2). Then different detection policies are formulated based on the burst state  $S^t[-1] \in \{1, 0\}$  that indicates whether the nearest time step  $t-1$  is bursty or not. When  $S^t[-1] == 0$ , the current workload is considered as burst if two conditions are satisfied: (i) there are proposal(s) suggested as burst in the nearest  $n$  proposals  $V^t[-n:]$ ; (ii) the nearest outlier information  $O^t[-1]$  shows that there are outlier(s) (Lines 3-4). When  $S^t[-1] == 1$ , the confidence of subsequent predictions is reduced by the influence of the burst. In this case, if either of conditions (i) and (ii) is satisfied, it is considered a burst (Lines 5-6). If it is still suggested to be non-burst, a further decision on whether it is a burst is made using a majority rule based on the nearest  $k$  ( $i$ ) proposals (Lines 7-10).

#### Algorithm 2 Pseudocode of Burst Detection

**Input:** Predicted workloads  $\hat{\mathbf{Y}}^t$ , ground truth workloads  $\mathbf{Y}^t$ , last  $k$  burst state  $S^t$ , nearest range length  $n$ , thresholds  $\lambda_d$  and  $\lambda_l$

**Output:**  $IsBurst$

- 1: Initialize  $D^t, O^t, L^t$  according to Eqs. (8), (9) and (12) with input  $\hat{\mathbf{Y}}^t$  and  $\mathbf{Y}^t$
- 2: Initialize  $V^t$  according to Eq. (13) with input  $D^t, O^t, L^t, \lambda_d$  and  $\lambda_l$
- 3: **if not**  $S^t[-1]$  **then**
- 4:   Set  $IsBurst = \sum V^t[-n:] > 0$  and  $O^t[-1] > 0$
- 5: **else**
- 6:   Set  $IsBurst = \sum V^t[-n:] > 0$  or  $O^t[-1] > 0$
- 7:   **if**  $IsBurst == 0$  **then**
- 8:     Remove the items in  $V^t$  with index  $i$  satisfying  $S^t[i] = 1$
- 9:     Set  $IsBurst = \sum V^t[-n:] \geq n/2$
- 10:   **end if**
- 11: **end if**
- 12: **return**  $IsBurst$

**Burst Handling.** If a burst is detected, the burst handler is designed to provide an appropriate overestimate of coming bursts, thus coping with the surge of user requests during bursts. In this component, we first use a second-order Autoregressive (AR) [39] to model the estimation of bursts. Unlike the *Informer*-based workload predictor that provides valuable insights into the data's long-term trends and global patterns, the AR model emphasizes capturing the local features of recent observations, thus better adapting to short-term dynamics during bursts. Specifically, an AR model has dynamics given by:

$$\hat{y}^{t+1} = c + \phi_1 y^t + \phi_2 y^{t-1} + \epsilon^t \quad (14)$$

where  $y^t = WL^t$  and  $y^{t-1} = WL^{t-1}$  are the inputs to the model representing the observed workloads at time  $t$  and  $t-1$ .  $\hat{y}^{t+1}$  is the model output representing the predicted workload at the future time  $t+1$ .  $c, \phi_1, \phi_2$  and  $\epsilon^t$  are the parameters, and  $\epsilon_t$  is assumed to be a white noise process.

Based on observations  $\{y^{t-L_z+1}, \dots, y^{t-1}, y^t\} \in \mathbb{R}^{L_z}$ , the parameters are optimized through *Maximum Likelihood Estimation*.

Since bursts tend to be a tiny part of overall workloads but have a considerable impact, proper overestimation helps to improve the robustness of burst handling. To achieve this, we add a residual term to the estimation by the AR model to generate an appropriate overestimate for bursts (Eq. (15)).

$$\hat{y}_{burst}^{t+1} = \hat{y}^{t+1} + U_{95\%CI}[Q_{95\%}(E^t)] \quad (15)$$

where  $U_{95\%CI}[\cdot]$  signifies the upper bound of the 95% confidence interval (CI) obtained through the bootstrap procedure, and  $Q_{95\%}(E^t)$  represents the 95th percentile of the residuals  $E^t$ .  $E^t$  is generated by:

$$E^t = \{y^j - \hat{y}^j \mid j \in [t-k+1, t]\} \quad (16)$$

TABLE 1  
State, Action and Reward of the DRL agent.

| State $S_t \in \mathcal{S}$  |
|--|
| Resource Utilization ( $RU_t$ ), Response Time ( $RT_t$ ),<br>Instances Number ( $IN_t$ ), Workload Feature ( $WF_t$ ) |
| Action $A_t \in \mathcal{A}_t^{p_t}$   |
| Origin Pivot Space $\mathcal{A}_t^{p_t^0}$ , Prediction Pivot Space $\mathcal{A}_t^{p_t^1}$                            |
| Reward $R_t \in \mathcal{R}$   |
| SLO Assurance Score ( $R_t^{RT}$ ), Resource Efficiency Score ( $R_t^{RU}$ )   |

### 3.4 Resource Estimator

Accurate resource planning of autoscaling plays a crucial role in optimizing system performance. Thus, we design the resource planner to find the right amount of resources (i.e., container-based instance replicas) for a cloud service/application to cope with coming workloads. It receives workload forecasts and outputs the recommended number of instances.

**Performance Modeling.** To achieve this, we first design a *Support Vector Regression* (SVR) [40] driven performance model to estimate the response time under given workloads and instance replicas. SVR, a powerful machine learning technique, is well-suited for performance modeling due to its ability to capture non-linear relationships. Our performance model is represented as following:

$$f_{SVR}(x) = w\phi(x) + b \quad (17)$$

where  $f_{SVR}(\cdot)$  denotes the predicted response time,  $x = \{IN, WL\}$  contains the workload intensity and number of instances.  $\phi(x)$  denotes the *Radial Basis Function* kernel applied to the input variables  $x$ , and  $w$  and  $b$  are the model parameters.

Historical data is collected from the target system to train the SVR model. These data consist of various workload scenarios and their corresponding response times. The workload scenarios cover different levels of workload intensity and resource quantities, with the workloads and resource quantities serving as the input variable and the response time as the output variable.

During the training phase, the SVR model aims to find an optimal hyperplane that maximizes the margin between

the predicted response times and the observed response times in the training data. This is achieved by using the *Sequential Minimal Optimization* (SMO) algorithm to solve the following optimization problem:

$$\begin{aligned} \min_{w,b} \quad & \frac{1}{2} \|w\|^2 + C\xi \\ \text{s.t.} \quad & |y_i - w_i x_i| \leq \epsilon + \xi, \xi \geq 0 \end{aligned} \quad (18)$$

where  $C$  is the penalty parameter for deviations from the margin,  $\epsilon$  is the margin width, and  $\xi$  are slack variables that allow for some training errors.

**Performance-Constrained Resource Estimation.** In the context of resource planning, the SVR-based performance model is utilized to determine the minimum resource quantities (i.e.,  $IN_{min}$ ) needed to meet an SLO-defined response time requirement  $\lambda_{RT}$ . Given the performance model  $f_{SVR}$  and a predicted workload  $WL_{pred}$ , the performance-constrained resource estimation can be expressed as the following:

$$IN_{min} = \min_{IN} \text{ s.t. } f_{SVR}(\{IN, WL_{pred}\}) < \lambda_{RT} \quad (19)$$

where  $WL_{pred} = \hat{y}_{burst}^{t+1}$  for bursts and  $WL_{pred} = \hat{y}_{median}^{t,1}$  for non-bursts. By iteratively adjusting the resource quantities and observing the corresponding predicted response times, we identified the optimal resource configuration that satisfies the response time constraint.

### 3.5 Estimation Enhancement

Compared to burst situations that require an appropriate overestimation strategy, non-burst situations require a more refined resource estimate. Thus, we design an RL agent, based on *Proximal Policy Optimization* (PPO) [41], to correct possible misestimations by the above method for non-bursts due to its ability to learn from experience and adapt dynamically to changing conditions. Specifically, at each discrete time step  $t = 1, 2, \dots$ , our RL formulation modeled as a *Markov Decision Process*  $(\mathcal{S}, \mathcal{A}, T, \mathcal{R}, \gamma)$ , where  $\mathcal{S}$  is a state space,  $\mathcal{A}$  is a set of actions available to an agent,  $T(s, a, s')$  is the (stochastic) transition function,  $\mathcal{R}$  is a reward space defined by reward function and  $\gamma \in [0, 1]$  is the discount factor. The goal of the RL agent is to optimize policy  $\pi_\theta$  to maximize the expected cumulative reward.

Table 1 shown the designed state, action, and reward of BAScaler at time  $t$ . The state  $S^t \in \mathcal{S}$  is designed as a tuple  $(RU^t, RT^t, IN^t, WF^t)$ . It contains the resource utilization of CPU  $RU^t$ , the response time  $RT^t$ , the number of instances  $IN^t$ , and the workload characteristics  $WF^t$  at the timestep  $t$ .  $WF^t$  contains the workload representation (described in §3.2) for the last  $k$  timesteps. The action  $A^t \in \mathcal{A}$  is fine-tuned based on the predicted instance number  $p_0^t = IN_{min}$  and current instance number  $p_1^t = IN^t$ :

$$\mathcal{A} = \mathcal{A}_{p_0^t}^t \cup \mathcal{A}_{p_1^t}^t; \mathcal{A}_{p_i^t}^t = \{p_i^t, p_i^t \pm 1, p_i^t \pm 2, \dots, p_i^t \pm \sigma\}; i \in \{0, 1\} \quad (20)$$

where  $\mathcal{A}_{p_i^t}^t$  represents the sub-action space based on  $p_i^t$ ,  $\sigma$  is used to control the fine-tuning range of the instance number. The reward  $R^t = \beta R_{RU}^t + (1 - \beta) R_{RT}^t$  is defined as a linear combination of  $R_{RT}^t$  and  $R_{RU}^t$  by using hyperparameter  $\beta \in$

$(0, 1)$ , where  $R_{RT}^t$  and  $R_{RU}^t$  are designed to measure SLO assurance and resource efficiency:

$$R_{RU}^t = \begin{cases} RU^t / \lambda_{RU}, & \text{if } RU^t \leq \lambda_{RU} \\ 2 - \frac{1 - \lambda_{RU}}{1 - RU^t}, & \text{else} \end{cases} \quad (21)$$

$$R_{RT}^t = \begin{cases} 1, & \text{if } RT^t \leq \lambda_{RT} \\ \alpha(\frac{\lambda_{RT}}{RT^t} - 2), & \text{else} \end{cases} \quad (22)$$

where  $\lambda_{RU}$  represents a CPU utilization threshold above which the QoS deteriorates rapidly, and  $\alpha$  is a penalty factor for response time violations.

## 4 EXPERIMENTAL EVALUATION

In this section, we evaluate BAScaler to answer following questions:

- **RQ1:** How effective is BAScaler?
- **RQ2:** How adaptive is BAScaler?
- **RQ2:** What is the contribution of each design in BAScaler?

### 4.1 Experimental Settings

**Benchmark Application.** Trend of cloud-native applications towards fine-grained tasks (as described in Section 2.2). To validate the autoscaling of fine-grained tasks, we employed a lightweight function service with millisecond-level response times that is sensitive to workload variations as a benchmark application. This service computes and outputs the discrete Fourier transform and its inverse for digital signals, representing a typical CPU-intensive application. We employed *Grafana K6*<sup>1</sup>, an open-source load testing tool, to generate concurrent digital signals, simulating specific workload traces to drive the service. Different workload traces were used to represent diverse active production environments, as detailed in the following paragraph.

**Workload Dataset.** We use ten different real-world workload traces derived from the top 10 ranked pages based on article pageviews in *Wikipedia* and its sister projects. These pages include *Barack Obama*, *Game of Thrones*, *Donald Trump*, *Elon Musk*, *2018 FIFA World Cup*, *Facebook*, *Elizabeth II*, *United States*, *YouTube*, and *Google*. These workloads encompass almost all the characteristics of real-world usage patterns, such as burstiness and seasonality. The workload data we used is publicly available<sup>2</sup> and maintained by the *Wikimedia Foundation*. To eliminate scale effects and thus compare the autoscaling performance across different workloads, we applied the *Z-Score* standardization to transform all workloads into a distribution with a mean of 500 and a standard deviation of 175. This transformation ensures the shape of original data distribution remains unchanged.

**Implementation Details.** We implemented *BAScaler* using Python 3.8, incorporating the implementation details and corresponding hyperparameter settings presented in Table 2. The underlying models for each component were developed utilizing open-source code, as indicated by the footnotes referencing the relevant resources. On this basis,

we proceeded to train the *Informer* model, SVR model, and RL agent associated with their respective components. This training process was conducted by invoking the corresponding APIs in the table, enabling us to prepare BAScaler for evaluation. Specifically, the *Informer* model was trained using the first 10,000 hours of data from each of the ten selected benchmark workload traces. The SVR model utilized historical data collected from the testbed for its training. The RL agent underwent training through interactive interactions with the testbed.

TABLE 2  
Implementation Details

| Component                             | Impl.  | Hyper-Parameter Settings  |
|---------------------------------------|--|---|
| Workload Predictor (§3.2)             | Informer <sup>3</sup>                                    | $L_x=720, L_y=168$  |
| Burst Detector & Burst Handler (§3.3) | Algo. 2<br>AR <sup>4</sup><br>Bootstrapping <sup>5</sup> | $k=24, n=3, \lambda_d=0.1, \lambda_l=0.1$<br>$\phi_1=2, \phi_2=-1, L_z=168$<br>iteration number = 100 |
| Resource Estimator (§3.4)             | SVR <sup>6</sup>   | kernel="rbf", $C=100$   |
| Estimation Enhancement (§3.5)         | PPO <sup>7</sup>   | $\gamma=0.99, \sigma=2, \beta=0.5, \lambda_{RU}=0.9$<br>$\lambda_{RT}=16ms, \alpha=1$                 |

**Baseline Autoscalers.** We implemented the following baselines as a comparison:

- **K8S-HPA** is Kubernetes' default horizontal pod autoscaler [42], which scales resources based on CPU utilization and a predefined threshold, representing the most widely used rule-based reactive approach.
- **A-SARSA** use an RL agent that fused predicted workloads into the state space to determine scaling action [43]. We chose A-SARSA because it represents the emerging RL-based predictive autoscaling approach.
- **BA-PA** is a burst-aware autoscaling approach that detects bursts in real-time based on statistical methods [44]. We compare BA-PA to evaluate the burst handling capabilities of BAScaler.

**Evaluation Metrics.** We primarily use the SLO violation rate and resource cost (i.e., the number of consumed Pods in Kubernetes) to evaluate the QoS assurance and resource consumption of the autoscaling algorithms. The SLO violation rate is the ratio of time steps violating the SLO to the overall time steps. Additionally, we use the number of request errors and response time variance to assess the loss of requests and the stability of response time, respectively. These metrics demonstrate better performance with smaller values.

### 4.2 Effectiveness Evaluation (RQ1)

To comprehensively validate the effectiveness of the proposed autoscaling method, we experiment with the pro-

<sup>3</sup>Informer [https://github.com/zhouhaoyi/Informer2020]

<sup>4</sup>AR [https://github.com/statsmodels/statsmodels]

<sup>5</sup>Bootstrapping [https://github.com/facebookarchive/bootstrapped]

<sup>6</sup>SVR [https://scikit-learn.org/stable/modules/generated/sklearn.svm.SVR.html]

<sup>7</sup>PPO [https://github.com/AI4Finance-Foundation/ElegantRL]

<sup>1</sup>Grafana K6 [https://github.com/grafana/k6]

<sup>2</sup>Wikimedia REST API [https://wikimedia.org/api/rest\_v1/]



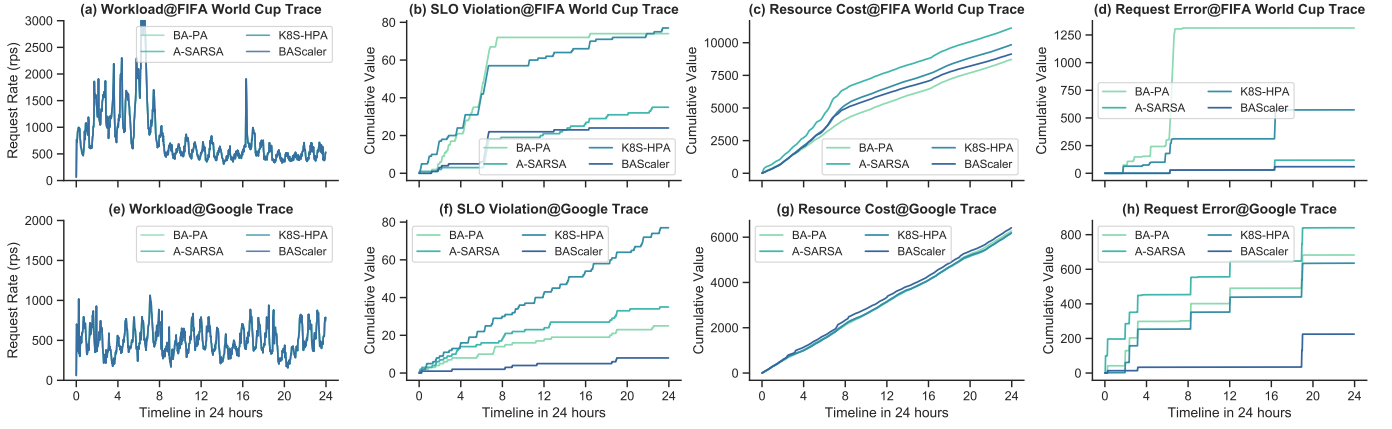


Fig. 6. Performance comparison on 2018 FIFA World Cup workload and Google workload.

posed approach with typical bursty and periodic workloads, each lasting 24 hours, and compared the results with baseline methods. The experiments are conducted on a Kubernetes cluster deployed on a public *Elastic Compute Service* (ECS) platform, with Kubernetes version v1.23.4. The testbed cluster comprised eight VMs running Ubuntu 18.04 LTS. Four VMs had 24 cores of CPU and 32 GB of memory, while the remaining four had 12 cores of CPU and 24 GB of memory. Istio service mesh with version 1.14.3 was employed to manage network traffic and to provide load balancing.

TABLE 3  
Quantitative result of the effectiveness evaluation

| Autoscalers | Metrics        |                 |               |                |
|-------------|----------------|-----------------|---------------|----------------|
|             | Violation      | Cost            | Error         | Variance       |
| BA-PA       | 6.9±3.4        | <b>10.4±1.7</b> | 998±315       | 3702±1271      |
| A-SARSA     | 4.9±0.0        | 12.0±3.4        | 479±361       | 1866±1327      |
| K8S-HPA     | 10.8±0.1       | 11.1±2.5        | 604±31        | 2196±65        |
| BAScaler    | <b>2.2±1.1</b> | 10.8±1.9        | <b>142±83</b> | <b>461±257</b> |
| Improvement | <b>67%±10%</b> | <b>3%±6%</b>    | <b>78%±6%</b> | <b>81%±59%</b> |

Fig. 6(a) depicts 2018 FIFA World Cup workload trace, demonstrating limited periodicity and burstiness, primarily focusing on World Cup-related activities and user behaviors. Figs. 6(b)-(c) respectively display the cumulative distribution of SLO violations, resource cost, and request errors for each autoscaler in the FIFA workload. The figures show that BAScaler exhibits the lowest SLO violations, request errors, and the second-lowest resource costs. These facts indicate that BAScaler can effectively handle stochastic and bursty workloads. We attribute this benefit to BAScaler’s burst detection and handling mechanism, which enacts a lenient resource allocation strategy based on the short-term trend of bursts. We also observe that BA-PA experiences higher SLO violations and request errors during burst periods despite having a configured burst detection and handling mechanism. That is because BA-PA relies on accurate resource estimation for bursts, but resource estimations during bursts are too tricky to be accurate.

Fig. 6(e) shows Google workload, which exhibits higher levels of periodicity and lower levels of bursts due to the

concentrated nature of user search requests within specific periods (e.g., weekdays and weekends). Figs. 6(f)-(h) respectively display the cumulative distribution of SLO violations, resource cost, and request errors for each autoscaler in the Google workload. These figures show that BAScaler significantly outperforms other methods regarding SLO violations and request errors, accompanied by almost consistent resource consumption. It indicates that BAScaler effectively handles periodic and predictable workloads. That is because BAScaler utilizes a range of advanced ML-based time series prediction methods and RL-based estimation enhancements, resulting in a more accurate resource estimation strategy than other autoscaler.

Table 3 summarizes the quantified experimental results of the above experiments, comparing different autoscalers applied to FIFA and Google workloads. The values before and after “±” denote each metric’s mean and standard deviation of the corresponding autoscaler across these two workloads<sup>8</sup>. From the table, we find BAScaler achieves an average reduction of 67% in SLO violation, a 3% decrease in resource cost, a significant 78% decrease in request error, and an 81% reduction in response time variance. These facts highlight the effectiveness and efficiency of BAScaler’s autoscaling capabilities in typical bursty and predictable workload scenarios.

### 4.3 Adaptability Evaluation (RQ2)

Here, we assess the adaptability of the proposed autoscaler to larger scales and more diverse workloads. The evaluation includes ten workload traces with different characteristics (described in §4.1), each with an increased data scale of 4000 hours. Conducting this experiment in a real-world Kubernetes platform is too time-consuming. Therefore, we conducted this experiment in a simulated environment based on CPU utilization and response time performance models. The construction and training of the performance models are detailed in §3.4. Once trained and validated, the performance models can predict the CPU utilization and response time for new workload scenarios. Fig. 7 illustrates the validation results of the performance models for 720

<sup>8</sup>In the following context, the values around “±” have the same meaning.

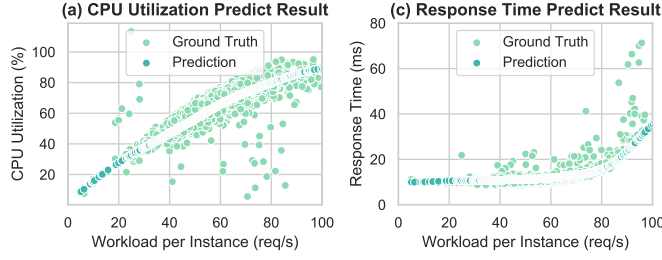


Fig. 7. Validation result of performance models

samples. It can be observed that the performance indicators predicted by the performance models fit the ground truth well. This means our Adaptability Evaluation conducted in the performance model-based simulation environment is reliable.

Fig. 8 presents the result of the adaptability evaluation conducted in the simulation environment, comparing the performance of baseline autoscalers under the ten workloads. The figure shows that BAScaler exhibits the most minor performance variability across different workloads, with performance metrics closely centered around the origin. This means that BAScaler can more efficiently and stably perform autoscaling under diverse workloads, indicating its superior adaptability to various workloads. In addition, the same autoscaler exhibits performance variations under different workloads, highlighting the necessity of adaptability evaluation for autoscaling.

Table 4 summarizes the quantified experimental results. The table shows that BAScaler outperforms other autoscalers across all three metrics. It reduces violation rate by an average of 57%, lowers resource cost by an average of 10%, and decreases response time variance by an average of 58%. Moreover, BAScaler demonstrates relatively tiny standard deviations in the corresponding metrics across different workloads, as indicated by the values following the  $\pm$ . These quantified metrics re-emphasize the superior adaptability of BAScaler.

TABLE 4  
Quantitative result of the adaptability evaluation

| Autoscalers | Metrics               |                       |                       |
|-------------|-----------------------|-----------------------|-----------------------|
|             | Violation Rate        | Resource Cost         | RT Variance           |
| BA-PA       | $2.51 \pm 2.75$       | $9.02 \pm 1.95$       | $5.56 \pm 4.27$       |
| A-SARSA     | $3.54 \pm 2.84$       | $12.78 \pm 8.69$      | $18.76 \pm 14.20$     |
| K8S-HPA     | $8.06 \pm 4.25$       | $8.67 \pm 2.60$       | $13.39 \pm 7.43$      |
| BAScaler    | $1.59 \pm 0.98$       | $8.85 \pm 2.69$       | $4.50 \pm 2.35$       |
| Improvement | $57.34\% \pm 17.88\%$ | $10.19\% \pm 14.63\%$ | $57.82\% \pm 24.89\%$ |

#### 4.4 Ablation Study (RQ3)

To analyze the contribution of each design in BAScaler, we conducted ablation studies building upon the foundation of adaptability evaluation experiments (§4.3). By selectively omitting specific modules of the proposed approach, we introduce three new autoscaling methods, which are as follows:

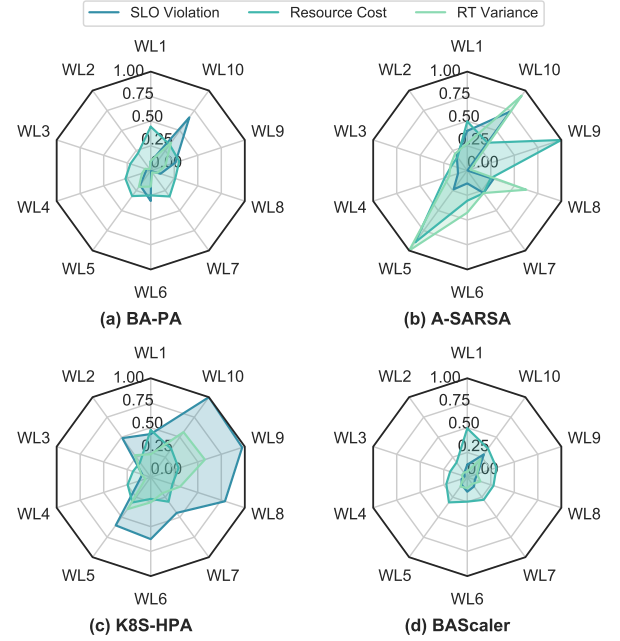


Fig. 8. Performance comparison on ten workloads with different characteristics. The results are normalized by using *Max-Min Normalization* and consistently setting the minimum value to 0.

- **Ab-Burst:** An ablation method for the burst detection and handling module, where all workloads allocate resources solely based on resource estimation and the estimation enhancement module.
- **Ab-Pred:** Ablation of the resource prediction module, implying an improvement in the reinforcement learning action space by not using resource prediction results in the RL action space, solely relying on the action space based on the current instance axis.
- **Ab-RL:** An ablation method for the reinforcement learning-based estimation enhancement module, allocating resources only based on the prediction results from the resource estimation module.

Fig. 9 presents the results of the ablation experiments. From the figure, we observed that BAScaler outperforms all ablation methods, indicating the effectiveness of each design in BAScaler. Specifically, (i) Ab-Burst exhibited a 1.7x increase in SLO violation and attained the highest response time variance at 3.6x, implying that the burst detection and handling module effectively manages bursty workloads, thereby controlling excessive response time and severe fluctuations. Additionally, Ab-Burst shows a slight 1% reduction in resource cost, attributed to the ablation of the burst handling module adopting a more relaxed resource allocation strategy for bursty workloads. (ii) Ab-Pred exhibited a 1.8x increase in SLO violation, a 2.0x increase in response time variance, and a marginal 4% increase in resource cost. It means that BAScaler's resource prediction module effectively predicts resources, guiding more efficient resource allocation. (iii) Ab-RL demonstrated a 1.4x increase in SLO violation, a 1.9x increase in response time variance, and a 1.3x increase in resource cost. It implies the presence of some inaccuracies in resource estimation in BAScaler, and the reinforcement learning-based estimation enhancement

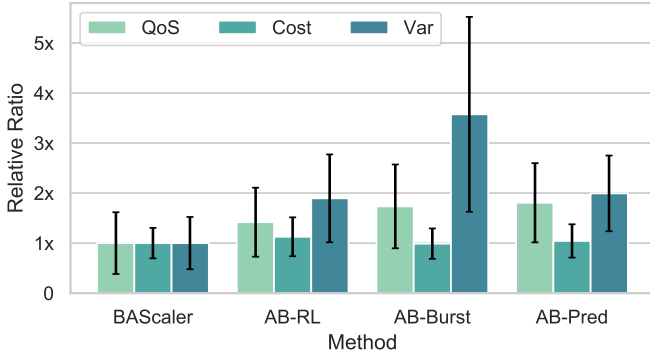


Fig. 9. Performance comparison of ablation methods.

module effectively corrects these erroneous estimates. It is attributed to the online learning capability of reinforcement learning, enabling real-time model adjustment based on the system's state. Compared to offline-trained resource estimation models, reinforcement learning proves more adept at adapting to dynamic changes in the system's environment.

## 5 DISCUSSION

**Applicability.** We employed a lightweight function service and its simulation to evaluate the effectiveness and adaptability of the proposed solution under various dynamic and unknown workloads. With proper customisation, the proposed solution can also be applied to applications composed of multiple services. To achieve this, we need to collect performance traces for each service and then reconfigure the relevant ML models for each submodule, enabling them to predict indicators for multiple services. This can be achieved by adjusting existing models (such as specifying multiple output layers for neural networks corresponding to different services) or replacing them with other models (such as graph neural networks). Additionally, a simpler approach is to deploy the solution independently for each service. However, this is only suitable for applications with a small number of services, as independent deployment in scenarios with numerous services may incur additional overhead.

The evaluation is focused on CPU-bound services; nevertheless, the proposed solution can also be applied to other resource-bound services. This is because the suggested approach adopts horizontal scaling with load balancing, where the minimum scaling unit is a container, and containers are configured with various resources required for the normal operation of the application.

**Limitations and Future Work.** First, while BAScaler's use of multi-level ML provides a robust and fine-grained approach to resource estimation, it relies on historical data for training. As a result, the quality and quantity of available historical data may limit the upper bound of BAScaler's performance.

Second, while BAScaler has illustrated outstanding results in guaranteeing QoS under dynamic workloads via fine-grained resource allocation, it may not be able to detect and mitigate other system anomalies that affect QoS (e.g., network congestion). Improving BAScaler by solving such

problems through online anomaly detection and handling is the future work.

Third, while BAScaler has demonstrated superior performance in handling dynamic workloads with different characteristics, the current study focused on autoscaling for user-facing cloud applications. It needs to be clarified how well BAScaler would perform in other types of cloud environments or for other types of applications. In the future, we will consider extremely heterogeneous and geographically distributed computation resources to improve BAScaler under hybrid clouds.

## 6 RELATED WORK

Autoscaling is an active research area in various cloud systems (e.g., databases, microservices, stream processing, and web applications). Recent surveys include [5], [20], [45]. They successfully applied autoscaling methods based on heuristics, queueing theory, control theory, and machine learning to their respective systems. Depending on the scaling timing, current autoscalings can be categorized into reactive and proactive methods.

**Reactive methods** focus on scaling resources in response to changes in workload or system conditions. These methods typically use threshold-based policies to trigger scaling actions when certain conditions are met. Major cloud platforms, such as *Amazon Web Service* and *Google Cloud*, use this technique. One notable example is Microscaler proposed by Yu et al. [8], which collects QoS metrics in the microservice infrastructure and utilizes a novel criterion called service power to determine the scaling-needed services. By combining online learning and a step-by-step heuristic approach, Microscaler achieves precise and optimal scaling decisions. While reactive methods excel in gradual and smooth workload changes, they may struggle with drastic fluctuations, resulting in under-provisioning and degradation of QoS.

**Proactive methods** enable proactive provisioning or de-provisioning of resources by anticipating future application needs. These methods leverage various techniques, such as time series analysis, deep learning, and reinforcement learning, to predict workload or resource usage and make scaling decisions in advance. Wang et al. [?] introduced DeepScaling, a proactive autoscaling approach that utilizes a three-step approach. It combines reinforcement learning for resource prediction, two deep neural networks for workload forecasting and CPU utilization estimation. By incorporating these innovative components, DeepScaling ensures stable resource utilization around the refined target level. However, proactive methods' effectiveness heavily relies on accurate predictions and is limited to predictable workloads with patterns, often struggling to handle random bursts commonly observed in certain applications.

**Hybrid Methods.** Some researchers have focused on the above problems of reactive and proactive methods in dynamic workloads. They propose hybrid approaches combining reactive and proactive strategies, allowing reactive scaling when proactive strategies fail. For example, Yan et al. [18] proposes a hybrid scaling method that contains an Bi-LSTM based proactive scaling module, a Kubernetes HPA based reactive scaling module and an reinforcement

learning based extended controller module. Where the extended controller module used to decide whether to adopt a proactive or reactive policy. Cheng et al. [46] proposed a hybrid approach that reactively offloads overloads to the cloud data center by setting a maximum queuing time and proactively provisioning microservice instances deployed on edge devices by predicting the result.

Compared to our work, these hybrid methods must be more robust as they generally lack consideration for workload bursts and may not effectively handle bursts. Furthermore, our approach integrates estimation results by carefully designing the DRL agent's multi-axis action space, enabling hybrid resource provision and fine-tuning resource allocation for more granular control.

## 7 CONCLUSION

In this paper, we present BAScaler, a burst-aware autoscaling approach, to manage the resource allocation of containerized cloud software services and applications on dynamic workloads for SLO assurance and cost efficiency. With the novel burst detection mechanism and multi-level ML models, BAScaler can better resolve bursts and estimate resources at a finer granularity. Compared with the SOTA autoscaling approaches, BAScaler obtains a more efficient resource allocation policy and significantly reduces SLO violations at a lower cost. The data and the implementation of BAScaler are publicly available at <https://github.com/SYSU-Workflow-Lab/Burst-Aware-Autoscaling>.

## ACKNOWLEDGMENTS

We express our sincere gratitude to the reviewers for their insightful comments and constructive suggestions, which significantly contributed to the refinement of this paper. This research is supported by the NSFC-Guangdong Joint Fund Project (Grant No. U20A6003), the National Natural Science Foundation of China (NSFC) (Grant No. 61972427), and the Research Foundation of Science and Technology Plan Project in Guangdong Province (Grant No. 2020A0505100030).

## REFERENCES

- [1] T. Chen and R. Bahsoon, "Self-adaptive and online qos modeling for cloud-based software services," *IEEE Transactions on Software Engineering*, vol. 43, no. 5, pp. 453–475, 2017. (document)
- [2] R. Buyya, S. N. Srirama, G. Casale, R. Calheiros, Y. Simmhan, B. Varghese, E. Gelenbe, B. Javadi, L. M. Vaquero, M. A. S. Netto, A. N. Toosi, M. A. Rodriguez, I. M. Llorente, S. D. C. D. Vimercati, P. Samarati, D. Milojicic, C. Varela, R. Bahsoon, M. D. D. Assuncao, O. Rana, W. Zhou, H. Jin, W. Gentzsch, A. Y. Zomaya, and H. Shen, "A manifesto for future generation cloud computing: Research directions for the next decade," *ACM Comput. Surv.*, vol. 51, no. 5, nov 2018. [Online]. Available: <https://doi.org/10.1145/3241737> (document)
- [3] Y. Al-Dhuraibi, F. Paraiso, N. Djarallah, and P. Merle, "Elasticity in cloud computing: State of the art and research challenges," *IEEE Transactions on Services Computing*, vol. 11, no. 2, pp. 430–447, 2018. (document)
- [4] Y. Li, Y. Lin, Y. Wang, K. Ye, and C. Xu, "Serverless computing: State-of-the-art, challenges and opportunities," *IEEE Transactions on Services Computing*, vol. 16, no. 2, pp. 1522–1539, 2023. (document)
- [5] C. Qu, R. N. Calheiros, and R. Buyya, "Auto-scaling web applications in clouds: A taxonomy and survey," *ACM Comput. Surv.*, vol. 51, no. 4, jul 2018. [Online]. Available: <https://doi.org/10.1145/3148149> 1, (document), 6
- [6] (2022) What is Auto Scaling? [Online]. Available: <https://www.alibabacloud.com/help/en/auto-scaling/product-overview/what-is-auto-scaling> (document)
- [7] T. Chen, R. Bahsoon, and X. Yao, "A survey and taxonomy of self-aware and self-adaptive cloud autoscaling systems," *ACM Comput. Surv.*, vol. 51, no. 3, jun 2018. [Online]. Available: <https://doi.org/10.1145/3190507> (document)
- [8] G. Yu, P. Chen, and Z. Zheng, "Microscaler: Cost-effective scaling for microservice applications in the cloud with an online learning approach," *IEEE Transactions on Cloud Computing*, vol. 10, no. 2, pp. 1100–1116, 2022. (document), 6
- [9] Z. Ding and Q. Huang, "Copa: A combined autoscaling method for kubernetes," in *2021 IEEE International Conference on Web Services (ICWS)*, 2021, pp. 416–425. (document)
- [10] V. Tadakamalla and D. Menasce, "Autonomic elasticity control for multi-server queues under generic workload surges in cloud environments," *IEEE Transactions on Cloud Computing*, 2020. (document)
- [11] M. Imdoukh, I. Ahmad, and M. G. Alfaiakawi, "Machine learning-based auto-scaling for containerized applications," *Neural Computing and Applications*, vol. 32, no. 13, pp. 9745–9760, 2020. (document)
- [12] E. Golshani and M. Ashtiani, "Proactive auto-scaling for cloud environments using temporal convolutional neural networks," *Journal of Parallel and Distributed Computing*, vol. 154, pp. 119–141, 2021. (document)
- [13] V. Rampérez, J. Soriano, D. Lizcano, and J. A. Lara, "Flas: A combination of proactive and reactive auto-scaling architecture for distributed services," *Future Generation Computer Systems*, vol. 118, pp. 56–72, 2021. (document)
- [14] H. Qian, Q. Wen, L. Sun, J. Gu, Q. Niu, and Z. Tang, "Robustscaler: Qos-aware autoscaling for complex workloads," in *2022 IEEE 38th International Conference on Data Engineering (ICDE)*, 2022, pp. 2762–2775. (document)
- [15] A. Bauer, N. Herbst, S. Spinner, A. Ali-Eldin, and S. Kounev, "Chameleon: A hybrid, proactive auto-scaling mechanism on a level-playing field," *IEEE Transactions on Parallel and Distributed Systems*, vol. 30, no. 4, pp. 800–813, 2019. (document)
- [16] X. Chen, L. Yang, Z. Chen, G. Min, X. Zheng, and C. Rong, "Resource allocation with workload-time windows for cloud-based software services: A deep reinforcement learning approach," *IEEE Transactions on Cloud Computing*, 2022. (document)
- [17] L. Schuler, S. Jamil, and N. Kühl, "Ai-based resource allocation: Reinforcement learning for adaptive auto-scaling in serverless environments," in *2021 IEEE/ACM 21st International Symposium on Cluster, Cloud and Internet Computing (CCGrid)*, 2021, pp. 804–811. (document)
- [18] M. Yan, X. Liang, Z. Lu, J. Wu, and W. Zhang, "Hansel: Adaptive horizontal scaling of microservices using bi-lstm," *Applied Soft Computing*, vol. 105, p. 107216, 2021. [Online]. Available: <https://www.sciencedirect.com/science/article/pii/S1568494621001393> (document), 6
- [19] F. Tahir, M. Abdullah, F. Bukhari, K. M. Almस्ताfa, and W. Iqbal, "Online workload burst detection for efficient predictive autoscaling of applications," *IEEE Access*, vol. 8, pp. 73 730–73 745, 2020. (document), 2.2
- [20] Z. Zhong, M. Xu, M. A. Rodriguez, C. Xu, and R. Buyya, "Machine learning-based orchestration of containers: A taxonomy and future directions," *ACM Comput. Surv.*, jan 2022, just Accepted. [Online]. Available: <https://doi.org/10.1145/3510415> (document), 6
- [21] M. I. Jordan and T. M. Mitchell, "Machine learning: Trends, perspectives, and prospects," *Science*, vol. 349, no. 6245, pp. 255–260, 2015. [Online]. Available: <https://www.science.org/doi/abs/10.1126/science.aaa8415> 2.1
- [22] M. Sugiyama, *Introduction to statistical machine learning*. Morgan Kaufmann, 2015. 2.1
- [23] Y. LeCun, Y. Bengio, and G. Hinton, "Deep learning," *nature*, vol. 521, no. 7553, pp. 436–444, 2015. 2.1
- [24] L. P. Kaelbling, M. L. Littman, and A. W. Moore, "Reinforcement learning: A survey," *Journal of artificial intelligence research*, vol. 4, pp. 237–285, 1996. 2.1
- [25] M. C. Calzarossa, L. Massari, and D. Tessera, "Workload characterization: A survey revisited," *ACM Computing Surveys (CSUR)*, vol. 48, no. 3, pp. 1–43, 2016. 2.1, 2.2
- [26] C. Reiss, J. Wilkes, and J. L. Hellerstein, "Google cluster-usage



traces: format+ schema," *Google Inc., White Paper*, vol. 1, pp. 1–14, 2011. 2.1

- [27] World cup web site access logs. [Online]. Available: <ftp://ita.ee.lbl.gov/html/contrib/WorldCup.html> 2.1
- [28] A. Ali-Eldin, J. Tordsson, E. Elmroth, and M. Kihl, "Workload classification for efficient auto-scaling of cloud resources," *Department of Computer Science, Umea University, Umea, Sweden, Tech. Rep*, 2013. 2.1
- [29] B. Abraham and J. Ledolter, *Statistical methods for forecasting*. John Wiley & Sons, 2009. 2.1
- [30] A. Ali-Eldin, O. Seleznev, S. Sjöstedt-de Luna, J. Tordsson, and E. Elmroth, "Measuring cloud workload burstiness," in *2014 IEEE/ACM 7th International Conference on Utility and Cloud Computing*, 2014, pp. 566–572. 2.1, 2.2
- [31] R. Gusella, "Characterizing the variability of arrival processes with indexes of dispersion," *IEEE Journal on Selected Areas in Communications*, vol. 9, no. 2, pp. 203–211, 1991. 2.1
- [32] T. N. Minh, L. Wolters, and D. Epema, "A realistic integrated model of parallel system workloads," in *2010 10th IEEE/ACM International Conference on Cluster, Cloud and Grid Computing*, 2010, pp. 464–473. 2.1
- [33] M. Vlachos, C. Meek, Z. Vagena, and D. Gunopulos, "Identifying similarities, periodicities and bursts for online search queries," in *Proceedings of the 2004 ACM SIGMOD International Conference on Management of Data*, ser. SIGMOD '04. New York, NY, USA: Association for Computing Machinery, 2004, p. 131–142. [Online]. Available: <https://doi.org/10.1145/1007568.1007586> 2, 2.2
- [34] D. Trihinas, Z. Georgiou, G. Pallis, and M. D. Dikaiakos, "Improving rule-based elasticity control by adapting the sensitivity of the auto-scaling decision timeframe," in *Algorithmic Aspects of Cloud Computing*, D. Alistarh, A. Delis, and G. Pallis, Eds. Cham: Springer International Publishing, 2018, pp. 123–137. 2.2
- [35] M. Lassnig, T. Fahringer, V. Garonne, A. Molfetas, and M. Branco, "Identification, modelling and prediction of non-periodic bursts in workloads," in *2010 10th IEEE/ACM International Conference on Cluster, Cloud and Grid Computing*, 2010, pp. 485–494. 2.2
- [36] A. Adegboyega, "Quantifying cloud workload burstiness: New measures and models," in *2017 IFIP/IEEE Symposium on Integrated Network and Service Management (IM)*, 2017, pp. 987–990. 2.2
- [37] (2022) Python client for the kubernetes api. [Online]. Available: <https://github.com/kubernetes-client/python> 3.1
- [38] H. Zhou, S. Zhang, J. Peng, S. Zhang, J. Li, H. Xiong, and W. Zhang, "Informer: Beyond efficient transformer for long sequence time-series forecasting," *Proceedings of the AAAI Conference on Artificial Intelligence*, vol. 35, no. 12, pp. 11 106–11 115, May 2021. [Online]. Available: <https://ojs.aaai.org/index.php/AAAI/article/view/17325> 3.2, 3.2
- [39] T. Bollerslev, "Generalized autoregressive conditional heteroskedasticity," *Journal of Econometrics*, vol. 31, no. 3, pp. 307–327, 1986. [Online]. Available: <https://www.sciencedirect.com/science/article/pii/0304407686900631> 3.3
- [40] M. Awad, R. Khanna, M. Awad, and R. Khanna, "Support vector regression," *Efficient learning machines: Theories, concepts, and applications for engineers and system designers*, pp. 67–80, 2015. 3.4
- [41] J. Schulman, F. Wolski, P. Dhariwal, A. Radford, and O. Klimov, "Proximal Policy Optimization Algorithms," *arXiv e-prints*, p. arXiv:1707.06347, Jul. 2017. 3.5
- [42] (2021) Horizontal pod autoscaling — kubernetes. [Online]. Available: <https://kubernetes.io/docs/tasks/run-application/horizontal-pod-autoscale/> 4.1
- [43] S. Zhang, T. Wu, M. Pan, C. Zhang, and Y. Yu, "A-sarsa: A predictive container auto-scaling algorithm based on reinforcement learning," in *2020 IEEE International Conference on Web Services (ICWS)*, 2020, pp. 489–497. 4.1
- [44] M. Abdullah, W. Iqbal, J. L. Berral, J. Polo, and D. Carrera, "Burst-aware predictive autoscaling for containerized microservices," *IEEE Transactions on Services Computing*, vol. 15, no. 3, pp. 1448–1460, 2022. 4.1
- [45] Y. Garí, D. A. Monge, E. Pacini, C. Mateos, and C. García Garino, "Reinforcement learning-based application autoscaling in the cloud: A survey," *Engineering Applications of Artificial Intelligence*, vol. 102, p. 104288, 2021. [Online]. Available: <https://www.sciencedirect.com/science/article/pii/S0952197621001354> 6
- [46] K. Cheng, S. Zhang, C. Tu, X. Shi, Z. Yin, S. Lu, Y. Liang, and Q. Gu, "Proscale: Proactive autoscaling for microservice with time-varying workload at the edge," *IEEE Transactions on Parallel and Distributed Systems*, pp. 1–18, 2023. 6



**Chunyang Meng** received his master degree from Beijing University of Posts and Telecommunications, China, in 2020. He is now a Ph.D. student at School of Computer Science and Engineering with Sun Yat-Sen University, China. His current research areas include distributed system, services computing, and AI driven operations. He was a recipient of the ACM SIGSOFT Distinguished Paper Award at ASE 2023 and the Best Student Paper Award at ICWS 2022.



**Haogang Tong** was born in 1995. He obtained his master's degree from Beijing University of Posts and Telecommunications in 2020. Currently, he is pursuing a Ph.D. degree at Sun Yat-sen University. He was a recipient of the ACM SIGSOFT Distinguished Paper Award. His research interests include microservices scheduling, edge computing, and the Internet of Things (IoT).



**Tianyang Wu** received the bachelor's and master's degrees in software engineering from the Sun Yat-sen University, Guangzhou, China, in 2020, and 2022 respectively. He is now working for Tencent Co. Ltd, China. His research interests include service computing, cloud computing and AI driven operations.



**Maolin Pan** received the B.S. degree from the Huazhong University of Science and Technology (HUST), Wuhan, China, in 1988, and the M.S. degree from HUST, in 1991, and the Ph.D. degree from Sun Yat-sen University (SYSU), Guangzhou, China, in 2017. He is currently a lecturer with the School of Software Engineering, SYSU. His research interests include BPM and workflow technical, cloud native computing.



**Yang Yu** received the bachelor's and master's degrees in computer science from the Huazhong University of Science and Technology (HUST), Wuhan, China, and the Ph.D. degree in computer science from Sun Yat-sen University (SYSU), Guangzhou, China, in 1988, 1991, and 2007, respectively. From 1991 to 2002, he was a Senior Engineer and CTO with a software company. From 2003, he became a Vice Professor with the School of Information Science and Technology at SYSU, where he has been a Full Professor with the School of Data and Computer Science and School of Software Engineering since 2011. He has published more than 90 papers and has been a reviewer for several prestigious international conferences and journals. He is a Distinguished Member of CCF and a member of ACM. His research interests include workflow/BPM, service computing, cloud computing, and software engineering.